

This is a self-archived version of an original article. This version may differ from the original in pagination and typographic details.

Author(s): Wu, Mengling; Zhang, Junle; Yuan, Liangqian; Rissanen, Kari; Pan, Fangfang

Title: Confinement Inside a Crystalline Sponge Induces Pyrrole to Form N–H π Bonded Tetramers

Year: 2021

Version: Accepted version (Final draft)

Copyright: © 2021 Wiley

Rights: In Copyright

Rights url: <http://rightsstatements.org/page/InC/1.0/?language=en>

Please cite the original version:

Wu, M., Zhang, J., Yuan, L., Rissanen, K., & Pan, F. (2021). Confinement Inside a Crystalline Sponge Induces Pyrrole to Form N–H π Bonded Tetramers. *Chemistry: A European Journal*, 27(38), 9814–9819. <https://doi.org/10.1002/chem.202100087>

Chemistry A European Journal

 **Chemistry
Europe**
European Chemical
Societies Publishing

Accepted Article

Title: Confinement Inside a Crystalline Sponge Induces Pyrrole to Form N-H... π Bonded Tetramers

Authors: Mengling Wu, Junle Zhang, Liangqian Yuan, Kari Rissanen, and Fangfang Pan

This manuscript has been accepted after peer review and appears as an Accepted Article online prior to editing, proofing, and formal publication of the final Version of Record (VoR). This work is currently citable by using the Digital Object Identifier (DOI) given below. The VoR will be published online in Early View as soon as possible and may be different to this Accepted Article as a result of editing. Readers should obtain the VoR from the journal website shown below when it is published to ensure accuracy of information. The authors are responsible for the content of this Accepted Article.

To be cited as: *Chem. Eur. J.* 10.1002/chem.202100087

Link to VoR: <https://doi.org/10.1002/chem.202100087>

WILEY-VCH

FULL PAPER

Confinement Inside a Crystalline Sponge Induces Pyrrole to Form N-H $\cdots\pi$ Bonded Tetramers

Mengling Wu,^{[a]‡} Junle Zhang,^{[b]‡} Liangqian Yuan,^[a] Kari Rissanen^{*[c]} and Fangfang Pan^{*[a]}

[a] Mengling Wu, Liangqian Yuan, Prof. Fangfang Pan,
Key Laboratory of Pesticide & Chemical Biology of Ministry of Education, Hubei International Scientific and Technological Cooperation Base of Pesticide and Green Synthesis, College of Chemistry
Central China Normal University
Luoyu Road 152, 430079 Wuhan, China
E-mail: fpan@mail.ccnu.edu.cn

[b] Junle Zhang
Henan Joint International Research Laboratory of Living Polymerizations and Functional Nanomaterials, Henan Key Laboratory of Advanced Nylon Materials and Application, School of Materials Science and Engineering
Zhengzhou University
450001 Zhengzhou, China

[c] Prof. Kari Rissanen
Department of Chemistry
University of Jyväskylä
P.O. Box 35, 40014 Jyväskylä, Finland
E-mail: kari.t.rissanen@jyu.fi

‡ These authors contributed equally to this work

Supporting information for this article is given via a link at the end of the document.

Abstract: Based on the DFT-level calculated molecular volume (V_{mol}) of pyrrole and its liquid density, pyrrole manifests the highest liquid density coefficient LD_c (defined as $[V_{\text{mol}} \cdot \text{density} \cdot 0.6023]/\text{FW}$) value of 0.7. Normal liquids have $LD_c < 0.63$. This very high LD_c is due to the strong N-H $\cdots\pi$ interactions in solution and hence pyrrole can be considered to be a pseudo-crystalline liquid. When trapped inside the confined space of the crystalline sponge a reorientation of the N-H $\cdots\pi$ interaction is observed leading to specific cyclic N-H $\cdots\pi$ tetramers and N-H $\cdots\pi$ dimers, verified by single crystal X-ray crystallographic and computational methods. These tetramers are of the same size as four pyrrole molecules in the solid-state of pyrrole, yet the cyclic N-H $\cdots\pi$ intermolecular interactions are circularly oriented instead of the linear zig-zag structure found in the X-ray structure of a solid pyrrole. The confinement thus acts as an external driving force for the tetramer formation.

Introduction

Molecular aggregation due to self-association is one of the most fundamental characters of chemical compounds.^[1] When it occurs, it affects the basic physical properties of the compound, such as chemical shift in the nuclear magnetic resonance (NMR) experiment, frequencies in rotational and vibrational spectra. Hence, the characterization of the self-aggregating behavior is generally done through NMR, microwave or infrared spectrum with the help of theoretical calculations.^[2] Single crystal X-ray crystallography, when successful, allows determination of the molecular assembling accurately at atomic level.^[3] However, the requirement of a good quality single crystal limits its applicability. A huge progress was made in the structure determination of liquids or non-crystalline substances in 2013^[4] thanks to the development of the crystalline sponge method (CSM),^[5] where the metal organic frameworks (MOFs) with permanent porosity was used to trap and orient the target molecules thus avoiding the

need of a single crystal of the target compound.^[4,5] Inspired by the CSM, we gathered if it would be possible to use it to study the intermolecular interactions and molecular aggregation of non-crystalline substances. Recently, we tried to form a halogen-bonded^[7] complex inside the channel of the ZnI_2 -TPT crystalline sponge,^[8] yet we observed that instead of forming the halogen-bonded complex, the halogen bond (XB) donors (diiodotetrafluorobenzene and diiodobenzene) tend to bind with the sponge framework walls, as they fit very well into the cavity and form C-I \cdots I-Zn halogen bonds.

We wondered what if a different type of XB acceptor would be used in conjunction with iodopentafluorobenzene (IPFB) as the XB donor. Due to its strong π -character that could potentially form XB with IPFB, we selected pyrrole. From another point of view, pyrrole is also considered as a pseudo-crystalline liquid^[9] because of the ubiquitous N-H $\cdots\pi$ interactions and the highest liquid density coefficient LD_c (defined as $[V_{\text{mol}} \cdot \text{density} \cdot 0.6023]/\text{FW}$) of 0.7. These features allow efficient self-aggregation via N-H $\cdots\pi$ even in diluted solutions.^[10] Once self-association occurs, the already known unsolvated crystal structure of pyrrole^[11] enables us to make detailed comparison. Furthermore, the interests in pyrrole also lie in the fact that the five member heterocycle is one of the most important subunits in both chemistry and biology.

In view of the above consideration, in this work we utilized the classical CS ZnX_2 -TPT ($X = \text{Cl}, \text{Br}, \text{I}$; TPT = 2,4,6-tri(4-pyridyl)-1,3,5-triazine) to "re-crystallize" the pyrrole-IPFB solution, and took the advantage of its confined space to either induce the XB interaction between pyrrole and IPFB, or re-orient the pyrrole molecules and direct the formation of some certain specific aggregations as happening in its liquid solution. The experimental results revealed that instead of forming the pyrrole-IPFB XB pair, the pyrrole and the XB donor molecules were separately distributed in the sponge channel. In detail, pseudo two-dimensional crystals of pyrrole form, where the unprecedented tetrameric cluster showing a cyclic geometry was constantly

FULL PAPER

present. Theoretical calculations also confirmed the preferred formation of the cyclic tetramer of pyrrole due to the strong synergic effect of the $\text{NH}\cdots\pi$ interactions.

Results and Discussion

Crystallography

The single crystals of the $\text{ZnX}_2\text{-TPT}$ ($X = \text{Cl}, \text{Br}, \text{I}$) sponge were obtained with the improved method.^[12] Before used for absorbing guests, the crystals were rinsed by chloroform and then soaked in the mixed solution of pyrrole and the XB donor. They were kept in the solution for three days, followed by the single crystal X-ray diffraction experiment at 100 K. After tens of tests, we found the the target guests can be readily adsorbed into the channels of CS, in particular with the help of the residual chloroform. Instead of forming the $\text{C-I}\cdots\pi$ XB pair, the pyrrole and the XB donor molecules were separately distributed in the sponge channel. Among others, in the case of **IPFB&PR@ZnI₂-TPT** (**IPFB**, **PR** = pyrrole), the pyrrole molecules distributed in a well ordered manner.

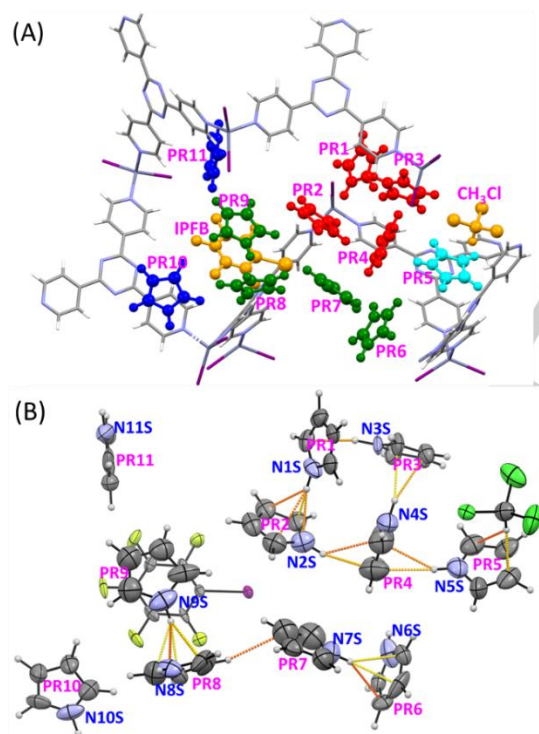


Figure 1. A) the distribution of the 11 symmetry-independent pyrrole molecules relative to the CS framework with the CS in capped sticks style and the guests in ball-and-stick; the pyrrole tetramer in red and the one together with the tetramer forming a pentamer in cyan, the two pyrrole dimers in green, the two “isolated” pyrrole in blue, and the chloroform and iodopenta-fluorobenzene in orange; only part of the CS framework around the 11 pyrrole was shown for clarity; B) the ORTEP plots showing the intermolecular interactions among the guests. The short interactions are shown as red and the long in yellow dotted lines

The structural analysis of **IPFB&PR@ZnI₂-TPT** indicated that the space group changed from the original $C2/c$ to $P2_1/c$ after trapping the guests. The symmetry breaking phenomenon was also observed when the crystal sponge was used to absorb molecular

iodine, where the same $P2_1/c$ space group was found.^[13] The $\text{ZnI}_2\text{-TPT}$ framework itself tends to maintain $C2/c$ space group symmetry (Figure S1), while the distribution of the guest molecules significantly deviates from the $C2$ axis and the center of inversion at $(1/2, 1/4, 1/4)$. Also the 90:10 disorder of the Zn and I atoms does not follow the $C2/c$ symmetry.

The asymmetric unit cell contains one chloroform, one IPFB and 11 independent pyrrole molecules, in addition to the six $-\text{ZnI}_2$ moieties connected by four TPT molecules forming the framework. The IPFB forms halogen bonds to $-\text{ZnI}_2$ site of the framework (ESI, Figure S2). It is extremely interesting to find that the 11 pyrroles are well ordered in the channel of the CS although there are no strong host-guest interactions to “lock” them (Figure 1A). This allows for the detailed determination of the intermolecular interactions and the relative orientation of the pyrrole molecules. The details of the structural analysis are documented in the SI. It should be noted that the N atoms of the pyrrole molecules have been assigned based on the largest electron density of the pyrrole ring (Figure S2, S3 and S4).

The 11 symmetry-independent pyrrole molecules can be divided into five groups, which contains five, two, two, one and one pyrrole molecules, respectively (Figure 1B). In the largest group, the five pyrroles are interacting with each other via $\text{N-H}\cdots\pi$ hydrogen bonds. Among them, four (PR1, PR2, PR3 and PR4) form a cyclic tetrameric pyrrole array. The fifth pyrrole (PR5) shows a $\text{N-H}\cdots\text{C}$ H-bond to the tetramer, while the chloroform interacts with the pyrrole P5 ring through its acidic hydrogen atom. The chloroform also shows weak $\text{C-Cl}\cdots\text{I}$ contact with a $\text{Cl}\cdots\text{I}$ separation of 3.590 Å and a $\text{C-Cl}\cdots\text{I}$ angle of 174.61° with the sponge framework (Figure 4 and S10-S15). Such contacts, despite being weak, were also found and played crucial role in the earlier reported structures.^[14] In addition, weak $\text{CH}\cdots\pi$ and $\text{CH}\cdots\text{I}$ interactions between the tetrameric cluster and the wall of CS were observed, which partially support and direct the cluster formation (Figure S16). One of the two pyrrole molecule groups (PR6 and PR7) is relatively “free” in the cavity with no significant contacts with the surrounding framework or other guests. The $\text{N-H}\cdots\pi$ hydrogen bond in the PR6-PR7 dimer results in a close to “T” shaped geometry, where the N-H of PR7 interacts with one of the carbon atoms of the PR6 with $\text{H}\cdots\text{C}$ distance of 2.408 Å and $\angle\text{N-H}\cdots\text{C}$ of 169.80°. The pyrroles PR8 and PR9 also interact via $\text{N-H}\cdots\pi$ bond to form a similar “T” shape with the N-H bond of PR9 pyrrole pointing to the center of the PR8 ($\text{H}\cdots\text{centroid}_{\text{pyrrole}} = 2.124$ Å, $\angle\text{N-H}\cdots\text{centroid}_{\text{pyrrole}} = 172.51^\circ$). A similar $\text{CH}\cdots\text{I}$ interaction between PR8 and the I-Zn-I group of the CS wall occurs (Figure S16). PR9 is partially stabilized through $\pi\cdots\pi$ interaction with the IPFB, which shows a weak halogen bond to the sponge wall ($R_{\text{XB}} = 0.902$). Thus the $\text{CH}\cdots\text{I}$ and $\pi\cdots\pi$ account for this dimer formation. It should be noted that the geometry of these dimers are different with that derived from the theoretical calculations (Figure S17). The two “isolated” pyrrole molecules (PR10 and PR11) reside relatively far away from the PR1 – PR9. PR10 and PR11 show multiple weak interactions with the framework walls, such as $\text{NH}\cdots\text{I}$ hydrogen bonds and $\text{CH}\cdots\pi/\pi\cdots\pi$ contacts.

FULL PAPER

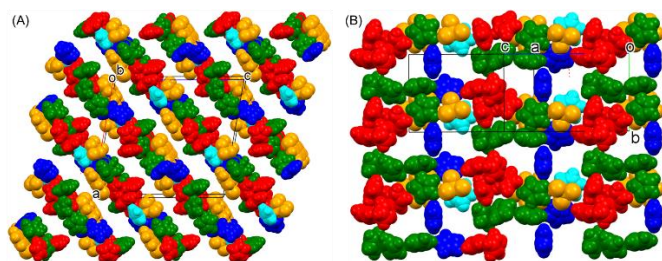


Figure 2. The orientation of the pyrrole molecules (CPK mode) in the channels of the CS along the crystallographic *b*-axis direction (A) and in (1 0 -1) plane (B) with the same color codes as in Figure 1A. The CS framework was excluded for clarity.

As described above, with the help of IPFB and chloroform, the CS guides and positions the pyrrole molecules into its two-dimensional channels (Figure 2).

The occurrence of the cyclic tetramer of pyrrole in the channel of the CS is unexpected. To probe this we then analysed the structures of two other similar systems, **IB&PR@ZnI₂-TPT** and **PR@ZnBr₂-TPT** (**IB** = iodobenzene). Surprisingly, the very similar pyrrole tetramers observed in **IPFB&PR@ZnI₂-TPT** and supported by the same pyrrole-chloroform pairs were detected in **IB&PR@ZnI₂-TPT** and **PR@ZnBr₂-TPT** (Figure 3). Contrary to **IPFB&PR@ZnI₂-TPT** these two CSs crystallized in the original space group *C2/c*, causing disorder of the pyrrole molecules inside the channels (Figure S5, S6).

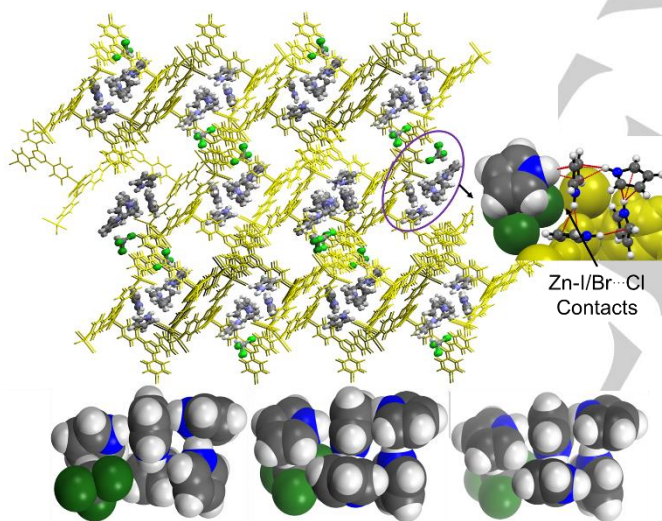


Figure 3. The re-oriented pyrrole tetramer in the crystalline sponge (top), and the CPK style plots of the cyclic tetramers supported by the chloroform-pyrrole pair in the structure of **IPFB&PR@ZnI₂-TPT** (left), **IB&PR@ZnI₂-TPT** (middle), and **PR@ZnBr₂-TPT** (right), respectively.

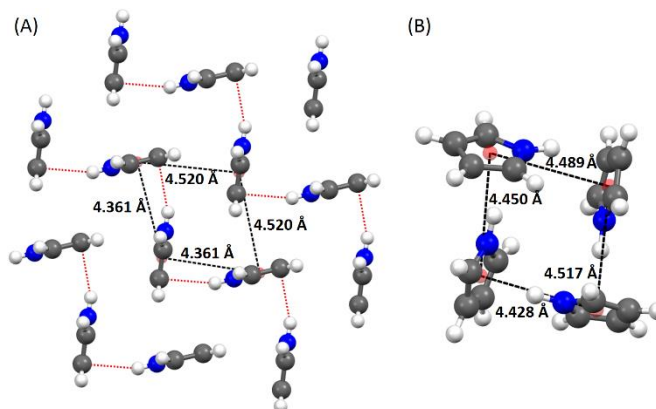


Figure 4. The pyrrole tetramer in the pyrrole crystal (A) and the comparison of the geometry of the tetrameric cluster of pyrrole in the **IPFB&PR@ZnI₂-TPT** (B) with the centroid-centroid distances labelled.

The intermolecular N-H \cdots π interactions between the pyrrole molecules in gas, pure liquid and unsolvated crystalline state have been confirmed previously.^[9-11] In its pure single crystalline form,^[11] the N-H \cdots π interactions link the pyrroles into a one-dimensional chain, which are packed together via van der Waals forces along the crystallographic *ac* plane (Figure S7-S10). Interestingly, a structurally similar cyclic tetramer can be located in the crystal lattice, but it is not a real tetramer, yet more like a 3 + 1 arrangement between two one-dimensional strands of the pyrrole molecules (Figure S8). As shown in Figure 4, the centroid to centroid distances of the neighboring pyrroles in the solid pyrrole and crystalline sponge are almost identical, varying from 4.36 to 4.52 Å. Accordingly, the tetramers take up nearly the same volume, 316.89 Å³ inside the CS (**IPFB&PR@ZnI₂-TPT**) and 317.48 Å³ in the solid^[11] pyrrole. The difference is that instead of four cyclic NH \cdots π interactions observed in CS, the two N-H \cdots π interactions supplemented with two weak C-H \cdots π in the solid pyrrole leads to a dense packing with *P_c* of 76.49%^[15] and resulting in a density of 1.17 g/cm³.^[11] All the intermolecular interactions in both structures were examined by the Hirshfeld surface analysis^[16] (Figure S10-S15).

As a comparison, we also calculated the *P_c* of pyrrole tetramer in the channel of the crystalline sponge. In the CS, the 11 pyrrole molecules take up around 1391.3 Å³ (with a probe of 1.2 Å calculated by *zeo++*^[16]). Given the molecular volume of the pyrrole molecule of 80.71 Å³, the *P_c* is 63.8% in the crystalline sponge, much higher than the 55% in the traditional supramolecular system proposed by Rebek.^[17] The liquid density coefficient *LD_c* for the pyrrole liquid is 0.7, much higher than for usual liquid solvents (Table S1), implying that the pyrrole molecules in the liquid pyrrole are spatially nearly as close together as they are in the solid pyrrole due to nearly as strong N-H \cdots π interactions. The lower density and *P_c* for all the CS-encapsulated pyrroles compared to the liquid pyrrole may be caused by the confinement effect of the nano-scale channel in the crystalline sponge.^[18] As for the pyrrole tetramer itself, the four pyrrole molecules pack as efficiently as those in the pyrrole crystal, since they show the similar geometry and the same volume and can be regarded as stable supramolecular clusters trapped inside the channels of the CS.

FULL PAPER

Computational Study

To have a deeper insight to the formation of the pyrrole clusters and the interactions between the pyrrole molecules, a series of geometry optimizations at the level of B97-3c combined with the single point energy calculation with M06-2X/def2-TZVPPD method using ORCA^[19] were performed. The average energy of an individual N-H \cdots π hydrogen bond in the pyrrole clusters was obtained by dividing the overall energy by the number of the N-H \cdots π hydrogen bonds in the cluster (Table S2). For the PR-IPFB system, the possible interactions including $\pi_{\text{PR}}\cdots\pi_{\text{IPFB}}$, N-H $\cdots\pi_{\text{IPFB}}$ and C-I $\cdots\pi_{\text{PR}}$ were also calculated. It was found that the $\pi_{\text{PR}}\cdots\pi_{\text{IPFB}}$ interaction (28.53 kJ/mol) was even stronger than the N-H $\cdots\pi$ in the pyrrole dimer (26.80 kJ/mol). The C-I $\cdots\pi_{\text{PR}}$ XB was slightly weaker (20.17 kJ/mol) and the N-H $\cdots\pi_{\text{IPFB}}$ was the weakest with an energy of only 4.54 kJ/mol (Figure S16). The calculated results agree with the crystallographic structures very well, where both the PR-IPFB $\pi\cdots\pi$ adduct and pyrrole clusters were observed. The Figure 5 and S17 show the results of the calculated pyrrole clusters, where the distance between the N-H and the adjacent pyrrole plane, as well as the average energy of the hydrogen bonds in each system were given.

As presented in Figure 5A, the close to "T" shaped dimer shown in the crystalline sponge tilts significantly after geometry optimization, giving a interplanar angle of 48.42° with an energy of 26.80 kJ/mol for the N-H $\cdots\pi$ hydrogen bond. The centroid to centroid distance of the two pyrrole molecules is 4.139 Å, almost the same with that found from the microwave spectroscopy (4.116 Å).^[20] The average values in the pyrrole dimer in CS and in the pyrrole crystal are 4.426 and 4.501, respectively. The calculations support

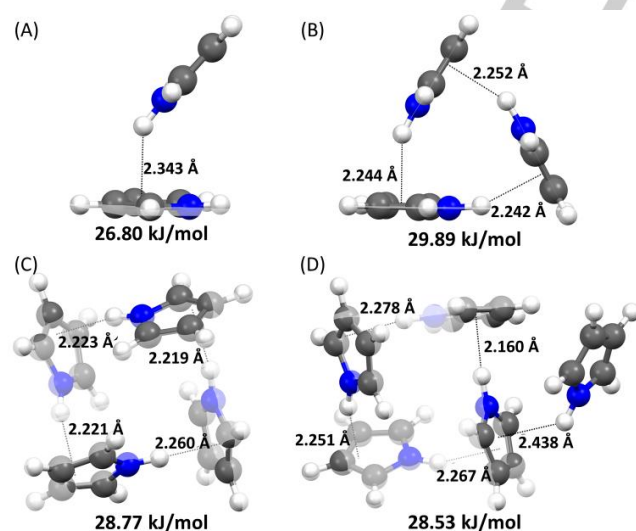


Figure 5. The calculated pyrrole dimer (A), trimer (B), tetramer (C) and pentamer (D). The dotted lines show the N-H $\cdots\pi$ hydrogen bonds with the distance between the hydrogen and the corresponding plane of the pyrrole. The average energy of the NH $\cdots\pi$ HB is indicated under each figure.

the hypothesis that by forming a cyclic trimer or tetramer structure the average energy of N-H $\cdots\pi$ hydrogen bonds

becomes stronger, indicating significant synergic effect (Figure 5B and 5C). The computational results show that the hydrogen bond interconnected pyrrole rings form cyclic tetramers, where each pyrrole acts as both HB donor and acceptor simultaneously. From computations the cyclic trimers appear to be most stable, but due to the sterical constrains due to available space, these trimers are not observed in the channels of all three crystal sponge structures. The pentamer can be considered as 4 + 1 orientation, but the N-H $\cdots\pi$ hydrogen bond between the monomer and the tetramer is much weaker than those within the tetramer as indicated by the 0.2 Å longer N-H $\cdots\pi$ H-bond (Figure 5D). These pentamers do exist in the CS structures and probably result in from the confinement effect of the CS framework and the higher stability of the cyclic tetramer.

Conclusion

In conclusion, three crystalline sponge were studied as flasks to "re-crystallize" pyrrole solution. It was found that pyrrole molecules re-orient themselves inside the channels of the ZnX₂-TPT sponges into very similar sub-structures as found in the pure solid pyrrole. Inside the CS the pyrrole molecules are pressed/guided/confined to primarily form N-H $\cdots\pi$ hydrogen-bonded dimers and tetramers. Interestingly, in all structures, IPFB&PR@ZnI₂-TPT, IB&PR@ZnI₂-TPT and PR@ZnBr₂-TPT, the formation of the cyclic pyrrole tetramers occurs when the ZnX₂-TPT framework and the two auxilliary molecules, viz. iodotetrafluorobenzene (IPFB) and chloroform were present. The IPFB molecules form additional "wall" component via I-I halogen bond to the iodine atom of the ZnI₂ moiety of the framework itself which is needed to form a suitable space for the pyrrole molecules to orient themselves. When comparing the spatial orientation of the pyrrole molecules in the channels of the CS with the same in pure solid pyrrole, it becomes evident that the confinement caused by the CS framework and auxilliary molecules directs the pyrrole molecules to adopt the unprecedented cyclic tetramer, yet reminiscent to the molecular packing of the solid pyrrole. The theoretical calculations imply that a strong synergic effect of the NH $\cdots\pi$ interactions in the cyclic tetramer is also an important factor. Accordingly, the pyrrole molecules in the tetrameric cluster pack as efficiently as in the unsolvated crystal.

This work demonstrates an efficient way to investigate how the spatial orientation of non-crystalline substrates and the molecular aggregating behavior is influenced by the weak intermolecular interactions supplemented by the confinement effects inside the channels of porous materials, especially crystalline sponges. Such aggregation and tight packing of the guests (same or different types) would be the basis of the potential reactions.^[25] In this regard, utilizing the interior surface of the MOF cavity to control the orientation of guests and guide the formation of some specific assembly would provide new possibilities for the supramolecular catalysis.

Experimental Section

General procedure for synthesis of the CS.

FULL PAPER

The sponge crystals of Zn₂-TPT and ZnBr₂-TPT were synthesized using the modified method according to the literature.^[12] In detail, 6.3 mg (0.020 mmol) tris(4-pyridyl)-1,3,5-triazine was dissolved in ca. 4 mL CHCl₃ by sonication. The solution was added to a 12 × 75 mm test tube. On top of this solution was layered carefully with 1 mL MeOH solution containing 9.6 mg Zn₂ (0.03 mmol) or 6.8 mg ZnBr₂ (0.03 mmol). The test tube was sealed and kept undisturbed at ambient conditions for three days. Colorless plate crystals were obtained on the wall of the test tube with the yield of ca. 60 %. The crystals were carefully taken from the test tube and washed with pure CHCl₃ to wash away the impurity.

Details of the crystallographic analysis

The data for crystals of IPFB&PR@Zn₂-TPT, IB&PR@Zn₂-TPT, and PR@ZnBr₂-TPT were collected at 100 K with a Rigaku XtaLAB AFC12 (RINC): Kappa single CCD using rotating-anode X-ray tube (Mo-K α , λ = 0.71073 Å) radiation. *CrysAlisPro*^[21] was used for both data collection and processing. The intensities were corrected for absorption using empirical method with spherical harmonics, implemented in SCALE3 ABSPACK scaling algorithm. The structures were solved with intrinsic phasing method in *SHELXT*^[22] and refined by full-matrix least-squares methods using the *OLEX2*,^[23] which utilizes the *SHELXL-2015* module.^[24] All non-hydrogen atoms in IPFB&PR@Zn₂-TPT were refined with anisotropic thermal parameters. While, for IB&PR@Zn₂-TPT and PR@ZnBr₂-TPT, part of the pyrrole molecules were kept isotropic due to the high disorder. The details of the treatment procedure were described in the supporting information. Deposition Number(s) 2009942 (for IPFB&PR@Zn₂-TPT), 2051584 (for PR@ZnBr₂-TPT), and 2051585 (for IB&PR@Zn₂-TPT) contain(s) the supplementary crystallographic data for this paper. These data are provided free of charge by the joint Cambridge Crystallographic Data Centre and Fachinformationszentrum Karlsruhe Access Structures service www.ccdc.cam.ac.uk/structures.

Computation details

The theoretical calculations were carried out with the program ORCA.^[19b] The B97-3c^[19a] method was used for the geometry optimization for all the aggregates including the pyrrole dimer, trimer, tetramer and pentamer, whose initial geometries were taken from the structure of IPFB&PR@Zn₂-TPT. The energy of the optimized models were calculated by meta-hybrid GGA DFT functionals M06-2X with the basis set of def2-TZVPPD. The overall energy of intermolecular interactions in each aggregation was obtained from the equation of $E_{\text{overall}} = E_{\text{aggregation}} - (E_{\text{monomer1}} + E_{\text{monomer2}} + \dots)$, then the average energy of the HB can be obtained by dividing the overall energy by the number of the HBs in the cluster. Details of the optimization results were listed in the supporting information.

Acknowledgements

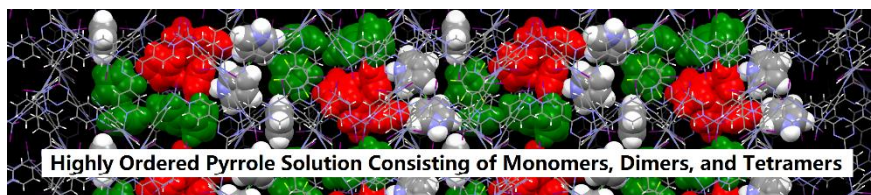
The authors gratefully acknowledge financial support from the National Natural Science Foundation of China (NSFC, F.P.: grant no. 21602071), and the Fundamental Research Funds for the Central Universities (F.P.: grant no. CCNU20QN010). This work was also supported by the Program of Introducing Talents of Discipline to Universities of China (111 program, B17019).

Conflict of interest

The authors declare no conflict of interest.

Keywords: aggregation • confinement effect • crystalline sponge method • host-guest chemistry • pyrrole tetramer

- [1] a) L. Gontrani, R. Caminiti, L. Bencivenni, C. Sadun, *Chem. Phys. Lett.* **1999**, *301*, 131-137; b) S. A. Kirillov, M. I. Gorobets, M. M. Gafurov, M. B. Ataev, K. Sh. Rabadanov, *J. Phys. Chem. B* **2013**, *117*, 9439-9448.
- [2] a) C. Dyllick-Brenzinger, G. R. Sullivan, P. P. Pang, J. D. Roberts, *Proc. Natl. Acad. Sci. U. S. A.* **1980**, *77*, 5580-5582; b) M. Bogdan, C. G. Floare, A. Pîrnau, *J. Phys.: Conf. Ser.* **2009**, *182*, 012002; c) S. A. Kulkarni, E. S. McGarrity, H. Meekes, J. H. ter Horst, *Chem. Commun.* **2012**, *48*, 4983-4985; d) B. T. G. Lutz, G. Astarloa, J. H. van der Maas, R. G. Janssen, W. Verboom, D. N. Reinhoudt, *Vib. Spectrosc.* **1995**, *10*, 29-40
- [3] a) L.-L. Ooi, *Principles of X-ray Crystallography*, Oxford Univ. Press, Oxford, **2010**, p. 176; b) G. M. Sheldrick, *Acta Crystallogr. Sect. A* **2008**, *64*, 112-122.
- [4] Y. Inokuma, S. Yoshioka, J. Ariyoshi, T. Arai, Y. Hitora, K. Takada, S. Matsunaga, K. Rissanen and M. Fujita, *Nature* **2013**, *495*, 461-466.
- [5] Y. Inokuma, T. Arai, M. Fujita, *Nat. Chem.* **2010**, *2*, 780-783.
- [6] a) S. Yoshioka, Y. Inokuma, M. Hoshino, T. Sato, M. Fujita, *Chem. Sci.* **2015**, *6*, 3765-3768; b) S. Urban, R. Brkljača, M. Hoshino, S. Lee, M. Fujita, *Angew. Chem. Int. Ed.* **2016**, *55*, 2678-2682; c) Q. Du, J. Peng, P. Wu, H. He, *TrAC, Trends Anal. Chem.* **2018**, *102*, 290-310.
- [7] G. R. Desiraju, P. S. Ho, L. Kloo, A. C. Legon, R. Marquardt, P. Metrangolo, P. Politzer, G. Resnati, K. Rissanen, *Pure Appl. Chem.* **2013**, *85*, 1711-1713.
- [8] L. Yuan, S. Li, F. Pan, *Inorg. Chem.* **2019**, *58*, 7649-7652.
- [9] W. J. Gee, *Dalton Trans.* **2017**, *46*, 15979-15986.
- [10] a) J. R. Ambrose, R. M. Hochstrasser, *J. Chem. Phys.* **1988**, *89*, 5956-5957; b) A. Lautie, A. Novak, *J. Chem. Phys.* **1972**, *56*, 2479-2481; c) J. A. Happe, *J. Phys. Chem.* **1961**, *65*, 72-76; d) L. Gontrani, F. Ramondo, R. Caminiti, *Chem. Phys. Lett.* **2006**, *417*, 200-205; e) M. Macchiagodena, G. Mancini, M. Pagliai, G. Cardini, V. Barone, *Int. J. Quantum Chem.* **2018**, *118*, e25554; f) Z. Gamba, M. L. Klein, *J. Chem. Phys.* **1990**, *92*, 6973-6974; g) W. T. Grubbs, T. P. Dougherty, E. J. Heilweil, *J. Phys. Chem.* **1995**, *99*, 10716-10722.
- [11] R. Goddard, O. Heinemann, C. Krüger, *Acta Crystallogr. Sect. C* **1997**, *53*, 1846-1850.
- [12] T. R. Ramadhar, S.-L. Zheng, Y.-S. Chen, J. Clardy, *Acta Crystallogr. Sect. A* **2015**, *71*, 46-58.
- [13] G. Brunet, D. A. Safin, M. Z. Aghaji, K. Robeyns, I. Korobkov, T. K. Woo, M. Murugesu, *Chem. Sci.* **2017**, *8*, 3171-3177.
- [14] a) K. Biradha, M. Fujita, *Angew. Chem. Int. Ed.* **2002**, *41*, 3392-3395; b) L. M. Hayes, C. E. Knapp, K. Y. Nathoo, N. J. Press, D. A. Tocher, C. J. Carmalt, *Cryst. Growth Des.* **2016**, *16*, 3465-3472.
- [15] The packing index here was calculated by $V_{\text{pyrrole}}/V_{\text{cell}}$. The space of one pyrrole molecule taking up in the solid pyrrole is 150.520 Å³, calculated via X-seed, and then the theoretical molecular volume of pyrrole of 80.71 Å³ gives rise to the Pc of 76.49%. The Kitaigorodskii type of packing index was 71.0% generated by PLATON after adjusting the C-H bond lengths to 1.079/1.081 Å and N-H length to 1.007 Å according to the EDF2/6-31G* optimized geometry for pyrrole.
- [16] D. Ongari, P. G. Boyd, S. Barthel, M. Witman, M. Haranczyk, B. Smit, *Langmuir* **2017**, *33*, 14529-14538.
- [17] S. Mecozzi, J. Rebek, Jr. *Chem. Eur. J.* **1998**, *4*, 1016-1022.
- [18] a) G. D. Stucky, J. E. Macdougall, *Science* **1990**, *247*, 669-678; b) G. Brunet, D. A. Safin, K. Robeyns, G. A. Facey, I. Korobkov, Y. Filinchuk, M. Murugesu, *Chem. Commun.* **2017**, *53*, 5645-5648.
- [19] a) J. G. Brandenburg, C. Bannwarth, A. Hanse, S. Grimme, *J. Chem. Phys.* **2018**, *148*, 064104; b) F. Neese, *WIREs Comput. Mol. Sci.* **2012**, *2*, 73-78; c) D. Rappoport, F. Furche, *J. Chem. Phys.* **2010**, *133*, 134105.
- [20] G. Columberg, A. Bauder, *J. Chem. Phys.* **1997**, *106*, 504-510.
- [21] *CrysAlisPro* 2018, Rigaku Oxford Diffraction. Version 1.171.39.46e
- [22] G. M. Sheldrick, *Acta Crystallogr. Sect. A* **2015**, *71*, 3-8.
- [23] O. V. Dolomanov, L. J. Bourhis, R. J. Gildea, J. A. K. Howard, H. Puschmann, *J. Appl. Crystallogr.* **2009**, *42*, 339-341.
- [24] G. M. Sheldrick, *Acta Crystallogr. Sect. C* **2015**, *71*, 3-8.
- [25] a) L. R. MacGillivray, G. S. Papaefstathiou, T. Friščić, T. D. Hamilton, D.-K. Bučar, Q. Chu, D. B. Varshney, I. G. Georgiev, *Acc. Chem. Res.* **2008**, *41*, 280-291; b) T. Murase, S. Horiuchi, M. Fujita, *J. Am. Chem. Soc.* **2010**, *132*, 2866-2867; c) C. G. P. Taylor, S. P. Argent, M. D. Ludden, J. R. Piper, C. Mozaceanu, S. A. Barnett, M. D. Ward, *Chem. Eur. J.* **2020**, *26*, 3054-3064.

Entry for the Table of Contents

An external driving force from the confined space of a crystalline sponge resulted in a reorientation of the N-H \cdots π interaction among pyrrole molecules. Such confinement effect led to the formation of pyrrole dimers and also the unprecedented clusters of cyclic tetramers. These results were verified by both single crystal X-ray crystallographic and computational methods.